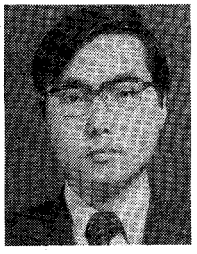

Takaaki Mukai was born in Osaka, Japan, on January 22, 1952. He received the B.S. and M.S. degrees in electronics engineering from Osaka University, Osaka, Japan, in 1975 and 1977, respectively.

In 1977 he joined the Musashino Electrical Communication Laboratory, Nippon Telegraph and Telephone Public Corporation, Tokyo, Japan. He has been engaged in research on the characteristics of semiconductor lasers and optical amplifiers.

Mr. Mukai is a member of the Institute of Electronics and Communication Engineers of Japan and the Japan Society of Applied Physics.

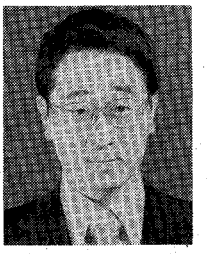

Yoshihisa Yamamoto (S'75-M'80) was born in Tokyo, Japan, on November 21, 1950. He received the B.S. degree from the Tokyo Institute of Technology, Tokyo, Japan, in 1973, and the S.M. and Ph.D. degrees from the University of Tokyo, Tokyo, Japan, in 1975 and 1978, respectively.

Since joining the Musashino Electrical Communication Laboratory, Nippon Telegraph and Telephone Public Corporation, Tokyo, Japan, in 1978, he has been engaged in research on photodetectors for optical communication, optical amplifiers, and coherent optical transmission systems.

Dr. Yamamoto is a member of the Institute of Electronics and Communication Engineers of Japan and the Japan Society of Applied Physics.

Optical FM Signal Amplification by Injection Locked and Resonant Type Semiconductor Laser Amplifiers

SOICHI KOBAYASHI, MEMBER, IEEE, AND TATSUYA KIMURA, SENIOR MEMBER, IEEE

Abstract—**Optical FM signal amplification by semiconductor lasers is studied by emphasizing their bandwidth characteristics. The laser is operated either in an injection-locked mode or in a resonant amplification mode by keeping the drive current above or just below its threshold.**

The bandwidths of both amplifiers are evaluated by the reduction in modulation sidebands and are compared with the bandwidths measured statically by scanning the frequency of incident CW wave. The $\sqrt{G}B$ = 25 GHz gain bandwidth product is obtained for both operation modes using a double heterostructure AlGaAs semiconductor laser.

The bandwidth obtained in the above procedure is in good agreement with theoretical results.

I. Introduction

COHERENT optical transmission systems, in which optical amplitude, frequency, or phase are modulated to carry information and are demodulated by heterodyne detection, are expected to improve optical fiber communication system performance, resulting in long repeater spacing and large information capacity [1]. The possibility of a coherent FM signal transmission system using a semiconductor laser transmitter and an independent local oscillator has successfully been demonstrated [2].

Important technologies related to a coherent FSK system have been studied using semiconductor lasers. Direct frequency modulation in a semiconductor laser has been studied theoretically and experimentally [3]. Semiconductor laser spectral line shape observation and linewidth reduction to less than 50 kHz, with an external grating feedback, have been reported [4]. Furthermore, single longitudinal mode operation of a semiconductor laser, directly modulated at a high data rate, has been realized by injection locking [5]. An injection-locked amplifier (ILA) and resonant type amplifier (RTA) performance using AlGaAs semiconductor lasers have also been studied for CW or AM modulated input [6], [7].

This paper reports on amplification of frequency modulated optical waves by semiconductor lasers operating in ILA and RTA modes. Evaluation of bandwidth characteristics for the two operation modes shows that the gain bandwidth product is given by $\sqrt{G}B$ = 25 GHz in a double heterostructure AlGaAs semiconductor laser. The bandwidth was measured by observing sideband amplitudes of frequency modulated waves at the input and output of the amplifier.

The above results on bandwidth are in good agreement with theoretical values. FM signal amplification was measured in microwave solid-state devices [8], [9]. Compared to these devices, the ILA operation of semiconductor lasers enables broad-band operation, since the carrier frequency is by far higher than that at microwaves. The ILA operation for a semiconductor laser, as well as the RTA operation, will be useful as devices for transmitters and receivers in future coherent optical transmission systems.

Manuscript received September 1, 1981; revised November 1, 1981.

The authors are with the Musashino Electrical Communication Laboratory, Nippon Telegraph and Telephone Public Corporation, Tokyo, Japan.

0018-9480/82/0400-0421$00.75

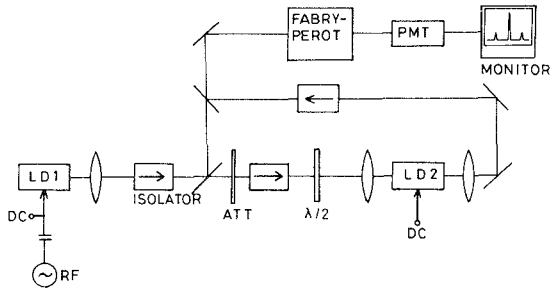

Fig. 1. Experimental setup for FM signal amplification measurement.

II. Experimental Setup and Procedure

A diagram of the experimental setup is shown in Fig. 1. Two double heterostructure AlGaAs semiconductor lasers (LD_1, LD_2) with an identical cavity length continuously operate in a single longitudinal mode at 840 nm. Both lasers are channeled-substrate-planar (CSP) geometry lasers. Their thresholds are $I_{th,1} = 62.3$ mA and $I_{th,2} = 60$ mA [10]. Both lasers are individually mounted on copper heat sinks whose temperatures are stabilized within $\pm 0.1^{\circ}$C accuracy by thermoelectric elements. Longitudinal mode frequency matching between the two lasers is carried out by the method reported previously [6].

The LD_1 output is injected into LD_2 through optical isolators. Two isolators are used in tandem for better isolation between two lasers. Isolators are also used to avoid undesired feedback from the Fabry-Perot interferometer to LD_1 and LD_2. The isolation is 25 dB. Spectra for both lasers are measured simultaneously by a Fabry-Perot interferometer, whose finesse is greater than 40 and free spectral range is about 4 GHz.

Both lasers are driven by dc bias currents. The magnitude of the LD_2 drive current, related to the threshold, depends on the mode of operation. An RF sinusoidal current is superimposed on the dc drive current of LD_1 and the FM wave is directly generated.

FM modulation by direct current modulation with an AlGaAs semiconductor laser was studied precisely in another paper in this special issue [14]. Frequency characteristics of FM efficiency from dc to 5 GHz and the mechanism of FM modulation by considering thermal and carrier effect were studied. Induced FM modulation by directly current modulation was heterodyne-detected by our co-worker, Dr. Saito, in a previous paper [3]. Frequency modulation indexes in the measurements are obtained by measuring the carrier and first sideband intensities using the scanning Fabry-Perot interferometer. Carrier and first sideband amplitude are calculated from the square root of observed sideband power spectra. The FM index is obtained from the ratio of first sideband amplitude to carrier. The first sideband has an asymmetric power according to the amplitude modulation components, so that the average value of both first sideband amplitudes are used. The effect of residual AM component is discussed in [14, Appendix]. A typical FM index is $\beta = 0.75$. Here, β stands for $\Delta F/f_m$, where ΔF is the frequency deviation and f_m is the modulation frequency. It was confirmed during the measurement that the FM index is in proportion to the RF drive current amplitude [3].

The input light is coupled to LD_2 by a microscope objective lens. The coupling loss, measured by the previously reported method [6], is typically 13 dB under no gain saturation condition. The optical gain is defined, as the power ratio of output and input light. Input light power P_i refers to the value measured in front of the input facet. Output power refers to that after the output facet. This, in contrast, is with the input power definition employed in the previous publication on semiconductor injection locking [6], in which the incident power referred to the value inside the input facet.

Static bandwidths of ILA and RTA are measured by injecting a CW signal into these amplifiers and by sweeping the input frequency by changing the LD_1 temperature. The dynamic bandwidths for these amplifiers are measured by injecting a directly modulated FM signal into these amplifiers and by comparing the FM indexes of input and output power spectra.

The optical bandwidth is defined by the modulation frequency at which the output and input FM index ratio β_{out}/β_{in} is equal to $1/\sqrt{2}$.

III. Experimental Results

A. Bandwidth of an Injection-Locked Amplifier

Locking bandwidth of ILA was measured by injecting a CW coherent light [6]. Fig. 2 shows the displayed power spectrum by scanning a single frequency CW input using the scanning Fabry-Perot interferometer. The frequency is scanned from high to low by varying the LD_1 drive current. Results on locking bandwidth versus locking gain are reproduced in Fig. 3 because the definition of gain is different from the previous publication [6]. The solid line curve shows the relation obtained from Adler's formula [11]. Hysteresis in the locking bandwidth was not measured for low input power shown in this figure.

Directly frequency modulated output from semiconductor laser (LD_1) is incident on LD_2 to measure the FM wave amplification. Fig. 4 shows typical input (a) and output (b) sideband spectra for -25 dBm input at 30 dB gain. Here, the modulation frequency is 500 MHz and the frequency modulation indexes are $\beta_{in} = 0.87$ and $\beta_{out} = 0.72$. The FM index is degraded by 17 percent through the amplification.

Fig. 5 shows the FM index ratio β_{out}/β_{in}, as a function of modulation frequency for several locking gain values. The gain was varied by changing the input power P_i, such as -42, -37, and -26 dBm, which corresponds to the gain values for the three series of experimental results shown in Fig. 5. Input FM index β_{in} is kept between 0.7 and 1.0. The locked laser is operated at 1.1 times the threshold. The solid theoretical lines will be discussed in Section IV.

When the modulation frequency is normalized by locking

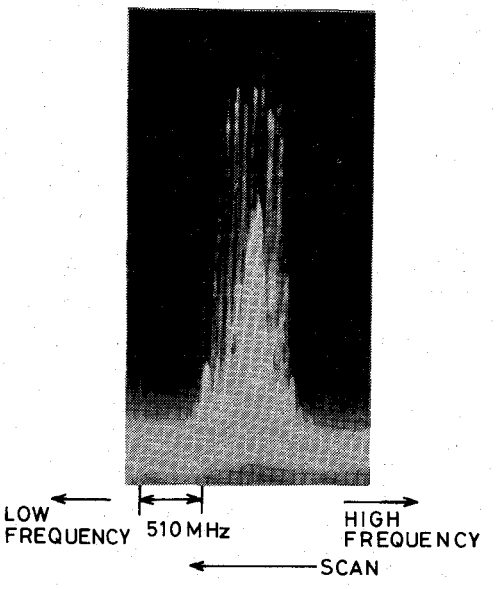

Fig. 2. Measured static locking bandwidth by scanning a single frequency CW input. The frequency is scanned from high to low by varying the LD_1 drive current. $\Delta f = 380$ MHz, $P_i = -27$ dBm, and $P_{I0} = 5.5$ dBm. Bias currents are $I_1 = 1.57 \times I_{th,1}$ and $I_2 = 1.25 \times I_{th,2}$. $I_{th,1} = 62.3$ mA and $I_{th,2} = 60$ mA.

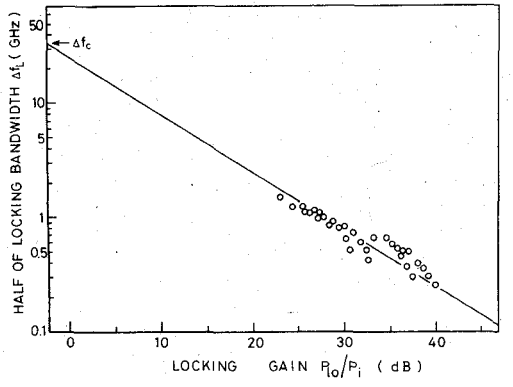

Fig. 3. Locking half bandwidth versus locking gain which is the ratio of an injection-induced laser power P_{I0} to injection power P_i measured outside the locked laser LD_2. ○: Experimental results [6]. Solid line shows the classical theory reported by Adler [11].

bandwidth Δf, the FM index ratio can be represented by a universal curve, as shown in Fig. 6. The ratio β_{out}/β_{in} degrades to $1/\sqrt{2}$, when f_m is equal to Δf. This shows the validity of the theory to be presented in Section IV.

B. Bandwidth of a Resonant Type Amplifier

When the laser LD_2 is operated at or slightly below its oscillation threshold, linear gain is available at a sufficiently low input level [12]. Amplification of frequency modulated optical waves is studied in an RTA mode operation of a semiconductor laser. The measurement method is the same as that for the ILA mode.

The bandwidth, measured in terms of β_{out}/β_{in} ratio, is shown in Fig. 7. The bias current levels of the LD_2 are 0.94, 0.98, and 1.0 times the threshold. Corresponding input power levels are -23, -26, and -26 dBm. Gain values obtained are 18, 23, and 25 dB. The input FM index is kept in the range of 0.7–1.0. Theoretical solid line curves will be discussed in the next section.

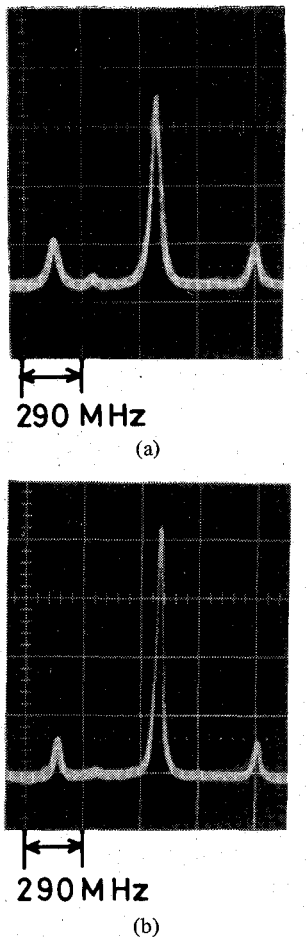

Fig. 4. Power spectra of directly frequency modulated signal observed by Fabry-Perot interferometer. Free spectral range (FSR) is 1.32 GHz and finesse is larger than 40. $f_m = 500$ MHz. $P_i = -25$ dBm. $I_2 = 1.35 \times I_{th,2}$. (a) Input power spectrum: $\beta_{in} = 0.87$. (b) Amplified output spectrum by ILA: $\beta_{out} = 0.72$. Locking gain P_{I0}/P_i is 30 dB.

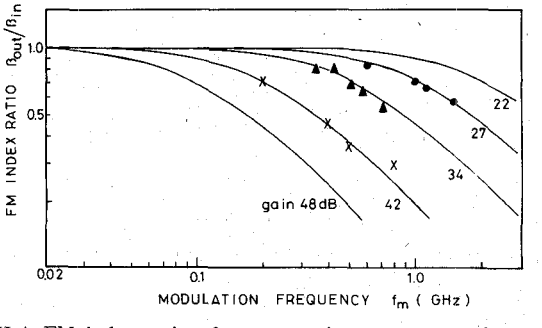

Fig. 5. ILA FM index ratio of output to input versus modulation frequency. Experimental results are obtained by the carrier and first sideband power spectra measured by FP interferometer. Input powers P_i are ×: -42 dBm, ▲: -37 dBm and ●: -26 dBm. Bias currents are $I_1 = 1.5 \times I_{th,1}$ and $I_2 = 1.1 \times I_{th,2}$. Solid line curves show calculated values by (3).

When the modulation frequency is normalized by the half bandwidth, $\Delta f_{1/2}$ at 3 dB down from the resonant peak gain in RTA (half width at half maximum–HWHM), the FM index ratio can be represented by a unified curve, as shown in Fig. 8. The ratio β_{out}/β_{in} degrades to $1/\sqrt{2}$, when f_m is equal to $\Delta f_{1/2}$. The HWHM $\Delta f_{1/2}$ will be discussed in the next section.

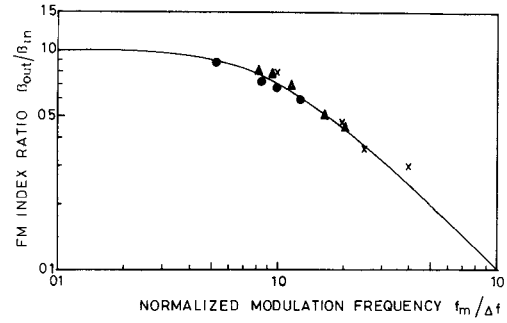

Fig. 6. ILA FM index ratio of output to input versus normalized modulation frequency by the locking half bandwidth Δf. Symbols are the same as in Fig. 5. The solid line curves shows values calculated by (3).

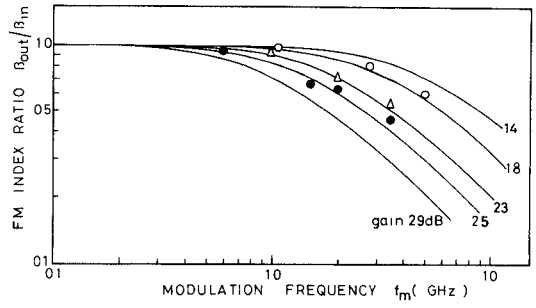

Fig. 7. RTA FM index ratio of output to input versus modulation frequency. Bias currents I_2 are ○: 0.94, △: 0.98, and ●: 1.0 times the threshold $I_{th,2}$. Input powers P_i are −23 dBm, −26 dBm, and −26 dBm, respectively. The solid line curves show values calculated by (4).

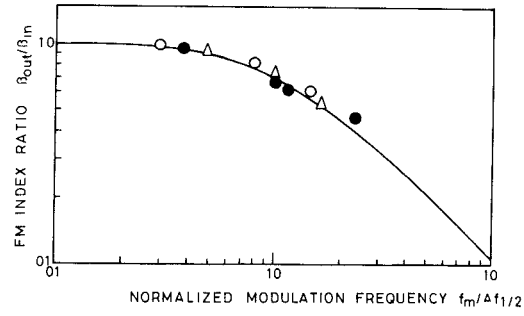

Fig. 8. RTA FM index ratio versus modulation frequency normalized by 3 dB down half bandwidth $\Delta f_{1/2}$. Symbols are the same as in Fig. 7. The solid line curve shows values calculated by (4).

IV. Discussion

A. Static Bandwidth and Saturation for Injection Locked and Resonant Type Amplifiers

Although the bandwidths of ILA and RTA modes have been reported in previous publications [6], [7], it will be useful to cite the results.

The injection-locking phenomenon has been explained by gain saturation [13]. The locking bandwidth is broadened as the input power increases. Locking half bandwidth Δf in Fig. 3 obeys the classical formula by Adler [11] as follows:

$$\Delta f = (1/4\pi\tau_p)\sqrt{P_{in}/P_l}\,. \tag{1}$$

Here, P_{in} and P_l mean input power and locked power in the laser cavity and τ_p is photon lifetime. Note that input power P_i in (1) refers to the power measured in the laser cavity and is

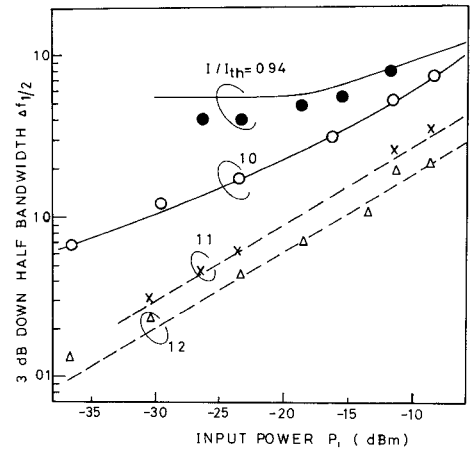

Fig. 9. Half bandwidth at 3 dB down of locked and resonant peak power versus input power P_i. CW light with a single longitudinal mode is injected into ILA and RTA. Broken line curves are calculated by substituting $\tau_p = 2.3 \times 10^{-12}$ s into (1). Solid line curves are values calculated by substituting $n = 3.6$, $L = 0.03$, and $R = 0.32$ into (2).

different from that defined in Section II by the function of the facet reflectivity.

The halfwidth $\Delta f_{1/2}$ of RTA is given by [7]

$$\Delta f_{1/2} = (c_0/2\pi nL)\sin^{-1}\{(1-R)/2\sqrt{G_r R}\}. \tag{2}$$

Here, c_0 is the light velocity in vacuum, n is the refractive index of the active layer, R is the laser amplifier facet reflectivity, and G_r is the resonant amplifier gain at the resonant peak frequency, which can be obtained experimentally [12].

To elucidate the saturation effect on the ILA and RTA bandwidths, the halfwidth has been measured as a function of input power. Fig. 9 shows $\Delta f_{1/2}$ at the amplifier output as a function of input power when the bias current is varied from 0.94-1.2 times the threshold. Experimental results are obtained by sweeping the CW optical frequency as shown in Fig. 3. Broken and solid curves show the values calculated by (1) and (2), respectively.

Experimental results are in good agreement with theoretical broken and solid curves. The slopes for RTA mode curves tend toward that for the ILA mode at high input levels. This is caused by the optical gain saturation in the active medium. Fig. 10 shows the HWHM as a function of the normalized bias current. The input levels are −26 dBm and −12 dBm. Broken and solid curves are values calculated from (1) and (2). This figure shows that, as the input level increases, the bias current dependence of the RTA mode approaches that of the ILA mode, again due to the gain saturation. The resonant gain G_r used in calculating (2), is depicted in Fig. 11. Here, input power P_i stands for the power measured outside the amplifier. The net gain coefficient per unit length g_l on the right ordinate is given by

$$g_l = (1/L)\ln G.$$

Here, G is the single-path gain and L is the cavity length. The amplifier gain becomes constant for input powers less than −25 dBm when the applied current is $0.94 \times I_{th,2}$. At threshold, the resonant amplifier gain saturates at −35 dBm input power. Experimental results at 0.94 and 0.98 in Fig. 7 are

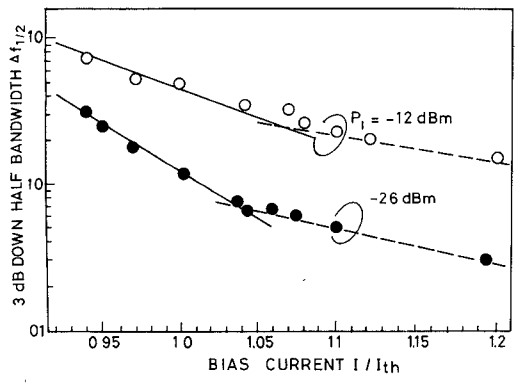

Fig. 10. Half bandwidth at 3 dB down from peak gain in ILA and RTA versus bias current. Broken and solid line curves are the same as in Fig. 9.

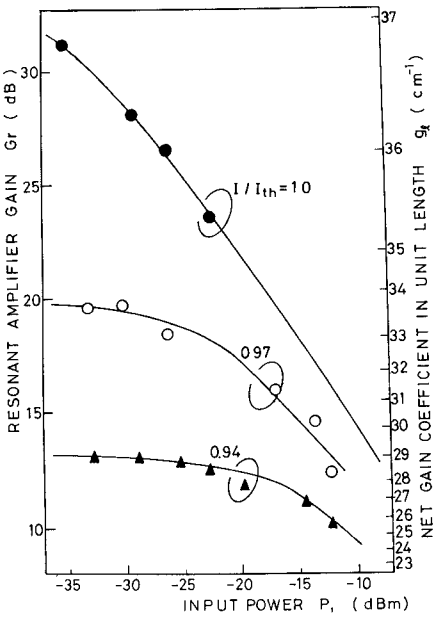

Fig. 11. RTA resonant gain versus input power. Input power is measured outside the RTA. Symbols show experimental results measured by sweeping the input frequency. Coupling loss is 13 dB measured at 0.94 times the threshold current under no gain saturation condition [6].

measured under unsaturated conditions, while the result at threshold is under the saturation conditions, as is seen from Fig. 11.

B. Spurious AM Modulation Effect in Resonant Type Amplifier

The directly modulated FM signal contains a spurious AM component [14]. We discuss, now, the AM modulation effect in the FM wave amplification.

Fig. 12 shows the AM modulation depth ratio M_{out}/M_{in} between input and output signals as a function of modulation frequency. AM modulation depth M is obtained from the ratio of carrier to first sideband amplitude. Experimentally obtained results are for bias current levels at 0.96, 0.99, and 1.0 times the threshold. The input power level is - 20 dBm. Solid curves from a to f are calculated by the first order perturbation rate equation combined with the van der Pol equation [15] assuming that $P_i = -20$ dBm, $\tau_p = 2$ ps and $\tau_s = 1$ ns

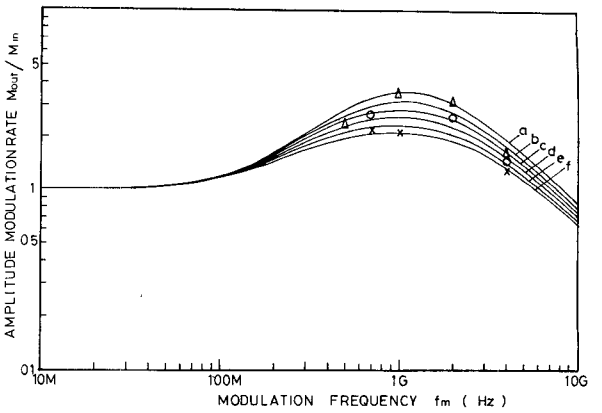

Fig. 12. Spurious AM index ratio in RTA versus modulation frequency. Symbols are experimental results obtained from the asymmetric upper and lower first sidebands, assuming that FM and AM modulations are out of phase with each other [14]. Bias currents are X : 0.96, O : 0.99, and Δ: 1.0 times the threshold, $I_{th,2}$. Solid line curves are calculated by the rate equation with the van der Pol equation (see the Appendix) under the same condition, as shown in Fig. 11. Bias currents are (a) 1.0, (b) 0.99, (c) 0.98, (d) 0.97, (e) 0.96, and (f) 0.95 times the threshold.

(see the Appendix). Amplitude modulation depth ratio M_{out}/M_{in} exceeds unity at about 1 GHz modulation frequency, when the resonant amplifier gain saturates in the RTA mode. The discrepancy between the experimental and calculated results in Fig. 12 is caused by an AM-FM conversion at about 1 GHz resonant frequency in RTA. A large input power saturates the amplifier gain when the RTA is biased close to threshold.

Fig. 13 shows the FM index ratio β_{out}/β_{in} for RTA at 1 GHz modulation frequency as a function of input power. Experimental results are for two bias current levels, 0.97 and 1.0 times the threshold. The solid curves show theoretical values (see the Appendix). The experimental results show a small peak at around - 23 dBm input, which cannot be explained by the theory. To understand the origin of this discrepancy, residual AM indexes for RTA input and output are studied from the asymmetry of upper and lower first sideband amplitude [14].

C. Bandwidth of Injection-Locked and Resonant Type Amplifiers

The theoretical curves in Figs. 5 and 6 for the ILA are obtained from a simplified van der Pol equation [8] as (3). Frequency deviation of the longitudinal mode in ILA is neglected. Detuning the bandwidth between the locked and the center frequency of the cold cavity in ILA is assumed to be very small:

$$(\beta_{out}/\beta_{in})_{ILA} = 1/\sqrt{1 + (f_m/\Delta f)^2}. \quad (3)$$

Here, the input FM index is assumed lower than 1.0. The half bandwidth Δf is the value obtained in Fig. 3. Experimental results in Figs. 5 and 6 show good agreement with the calculated value.

RTA theoretical curves in Figs. 7 and 8 are calculated from (2) assuming that the input FM index is small, as follows:

$$(\beta_{out}/\beta_{in})_{RTA} = 1/\sqrt{1 + (f_m/\Delta f_{1/2})^2}. \quad (4)$$

Here, $\Delta f_{1/2}$ is the HWHM with CW optical injection in RTA.

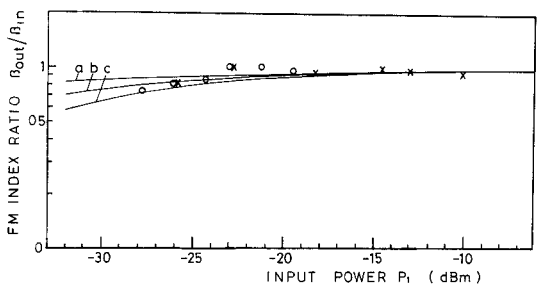

Fig. 13. Input power dependence of FM index ratio in RTA. Bias currents are X: $0.97 \times I_{th,2}$, O: $1.0 \times I_{th,2}$. Solid line curves are values calculated by the rate equation, combined with the van der Pol equation (see the Appendix) when detuning is nearly zero, $\beta_{in} = 0.73$ and input AM index is 5 percent.

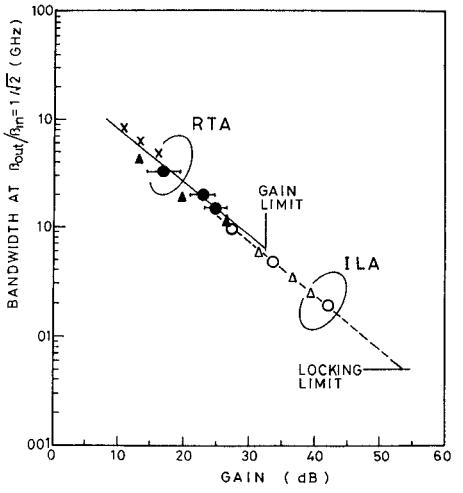

Fig. 14. Bandwidth versus gain characteristics for ILA and RTA. Bandwidths measured with FM signals are indicated by O: ILA and ●: RTA. The bandwidth is depicted by $\beta_{out}/\beta_{in} = 1/\sqrt{2}$. Bandwidths measured by frequency swept CW wave are indicated by Δ: ILA, ▲: RTA ($P_i = -26$ dBm) and X: RTA ($P_i = -12$ dBm). Broken and solid lines are calculated by (1) and (2). Experimental and calculated results show $\sqrt{G}B = 25$ GHz for ILA and RTA.

Fig. 14 shows HWHM for ILA and RTA for CW and FM signal input as a function of the amplifier gain. The experimental results in Figs. 5, 7, and 8 are replotted in this figure. The broken and solid lines are obtained from Figs. 3 and 4, respectively.

This figure shows that the gain bandwidth product for both ILA and RTA modes are given approximately by $\sqrt{G}B = 25$ GHz. The RTA is suitable for relatively low gain and broad-band operation, whose maximum gain is imposed by the gain at a threshold around 30 dB. The ILA is suitable for high gain and relatively narrow bandwidth operation, whose bandwidth is limited by the center frequency fluctuation at around 50 MHz.

To obtain the large gain bandwidth product $\sqrt{G}B$, small reflectivity R and short cavity length L are effective for both ILA and RTA. The reduced cavity Q value, however, may increase AM and FM noises in these amplifiers. The development of optimum design criteria for optical amplifiers, with respect to the gain bandwidth product as well as noise, is necessary.

The RTA will be successful for broad-band repeater amplifiers, while the ILA will be useful for high power and relatively narrow band post amplifiers [1].

V. Conclusion

Frequency modulated optical wave amplification was studied in injection-locked and resonant type amplifiers using double heterostructure semiconductor lasers. Bandwidths for the two types of amplifiers were measured by measuring the sideband amplitude of amplified FM waves over a wide modulation frequency. The gain bandwidth product of $\sqrt{G}B = 25$ GHz is obtained for both modes of operation, in good agreement with theory. FM-AM conversion in RTA at high input level may cause deviation from the theory. The ILA mode is suitable for high gain and high output level operation, while the RTA mode is suitable for broad-band operation.

Appendix

Rate equation combined with the van der Pol equation, assuming that gain is in direct proportion to electron density and spontaneous term is neglected, are given as follows [15]:

$$dn/dt = (I - n - nS_l)/\tau_s \tag{A1}$$

$$dE_l/dt = (n - 1)E_l/2\tau_p - E_{in}\cos(\Psi - \Phi)/2\tau_p \tag{A2}$$

$$d\Phi/dt = (E_{in}/E_l)\sin(\Psi - \Phi)/2\tau_p - \Delta\omega + d\theta/dt \tag{A3}$$

$$I = J/J_{th}$$

$$S_l = \tau_s S/(\tau_p N_{th} v_a) = E_l^2$$

$$P_{in} = \tau_s P/(\tau_p N_{th} v_a) = E_{in}^2$$

$$n = N/(\tau_p \chi J_{th}) = N/N_{th}$$

$$\chi = 1/ed$$

$$\Delta\omega = \omega_{in} - \Omega_0 (= \omega_l - \Omega_0).$$

Here, J is the current density, S is the photon density, τ_s is carrier recombination time, τ_p is photon lifetime, N is the electron density, v_a is the active region volume, d is active layer thickness, e is electron charge, P is the injected photon density, E_l is the locked electric field amplitude, E_{in} is the injected electric field amplitude, ω_{in} is injection light angular frequency, ω_l is locked angular frequency, and Ω_0 is the center angular frequency of the resonator of LD_2. In injection-locked state, $\omega_{in} = \omega_l$. Subscript indicated by th means threshold state value. Φ is the phase of locked signal, θ is the phase of free running laser (LD_2), and Ψ is the phase of injection signal from LD_1.

First-order perturbation of rate equation is obtained from (A1), (A2), and (A3) assuming as follows:

$$S_l = S_0 + S_1 = E_0^2 + 2E_1E_0$$

$$E_l = E_0 + E_1, E_{in} = E_{i0} + E_{i1}$$

$$n = n_0 + n_1$$

$$I = I_0 + I_1$$

$$\phi = \phi_0 + \phi_1$$

$$\Phi = \Phi_0 + \Phi_1$$

$$\Psi = \Psi_0 + \Psi_1. \tag{A4}$$

Here, various suffixes for 0 and 1 mean dc and first-order perturbation. Substituting (A4) into (A1), (A2), and (A3), first-order perturbation rate equation is obtained as follows:

$$j\omega n_1 = (I_1 - n_1 - n_1 E_0^2 - 2n_0 E_1 E_0)/\tau_s \tag{A5}$$

$$j\omega E_1 = [(n_0 - 1)E_1 + E_0 n_1 - \{E_{i1}\cos(\Psi_0 - \Phi_0) - E_{i0}(\Psi_1 - \Phi_1)\sin(\Psi_0 - \Phi_0)\}]/2\tau_p \tag{A6}$$

$$j\omega\Phi_1 = [\{E_{i1}\sin(\Psi_0 - \Phi_0) + E_{i0}(\Psi_0 - \Phi_0) \cdot \cos(\Psi_0 - \Phi_0)\}/2\tau_p - \Delta\omega E_1 - j\omega\theta_1 E_0]/E_0. \tag{A7}$$

The dc equations are obtained from (A1), (A2), and (A3), as follows:

$$0 = I_0 - n_0 - n_0 S_0 \tag{A8}$$

$$0 = (n_0 - 1)E_0/2\tau_p - E_{i0}\cos(\Psi_0 - \Phi_0)/2\tau_p \tag{A9}$$

$$0 = (E_{i0}/E_0)\sin(\Psi_0 - \Phi_0)/2\tau_p - \Delta\omega. \tag{A10}$$

From (A9) and (A10), we obtain

$$(n_0 - 1)E_0^2 + (2\tau_p)^2 E_0^2 \Delta\omega^2 = E_{i0}^2. \tag{A11}$$

By substituting (A8) into (A11), nonlinear power equation in injection locking is as follows:

$$\{I_0/(1 + S_I) - 1\}^2 S_I + \Delta\omega^2 4\tau_p^2 S_I = P_{\text{in}}, \tag{A12}$$

where

$$S_I = E_0^2 \text{ and } P_{\text{in}} = E_i^2.$$

The solid line curves in Fig. 12 are obtained as $(E_1/E_0)/(E_{i1}/E_{i0})$ from (A5)-(A10) under the condition that $\tau_p = 2$ ps, $\tau_p = 1$ ns, $\Delta\omega \cong 0$, $\theta_1 \cong 0$, $\Phi_1 \cong 0.73$, and $(E_{i1}/E_{i0})^2 = 10$. The solid line curves in Fig. 13 are obtained as Φ_1/Ψ_1 from (A5)-(A10) under the same condition.

Acknowledgment

The authors wish to thank Dr. Y. Yamamoto and T. Mukai for stimulating discussion and suggestion.

References

[1] Y. Yamamoto and T. Kimura, "Coherent optical fiber transmission systems," *IEEE J. Quantum Electron.*, vol. QE-17, pp. 919-935, June 1981.

[2] S. Saito, Y. Yamamoto, and T. Kimura, "Optical FSK heterodyne detection experiments using semiconductor laser transmitter and local oscillator," *IEEE J. Quantum Electron.*, vol. QE-17, pp. 935-941, June 1981.

[3] S. Kobayashi, Y. Yamamoto, and T. Kimura, "Modulation frequency characteristics of directly optical frequency modulated AlGaAs semiconductor laser," *Electron. Lett.*, vol. 17, pp. 350-351, May 1981.

[4] S. Saito and Y. Yamamoto, "Direct observation of Lorentzian lineshape of semiconductor laser and linewidth reduction with external grating feedback," *Electron. Lett.*, vol. 17, pp. 325-327, Apr. 1981.

[5] S. Kobayashi, J. Yamada, S. Machida, and T. Kimura, "Single-mode operation of 500 Mbit/s modulated AlGaAs semiconductor laser by injection locking," *Electron. Lett.*, vol. 16, pp. 746-748, Sept. 1980.

[6] S. Kobayashi and T. Kimura, "Injection locking in AlGaAs semiconductor laser," *IEEE J. Quantum Electron.*, vol. QE-17, pp. 681-689, May 1981.

[7] T. Mukai and Y. Yamamoto, "Gain, frequency bandwidth, and saturation output power of AlGaAs DH laser amplifier," *IEEE J. Quantum Electron.*, vol. QE-17, pp. 1028-1034, June 1981.

[8] T. Isobe and M. Tokida, "A new microwave amplifier for multichannel FM signal using a synchronized oscillator," *IEEE J. Solid-State Circuits*, vol. SC-4, pp. 400-408, Dec. 1969.

[9] M. Heines, J. C. Collinet, and J. G. Ondria, "FM noise suppression of an injection phase-locked oscillator," *IEEE Trans. Microwave Theory Tech.*, vol. MTT-16, pp. 738-742, Sept. 1968.

[10] M. Nakamura, K. Aiki, N. Chinone, R. Ito, and J. Umeda, "Longitudinal-mode behavior of mode-stabilized $Al_xGa_{1-x}As$ injection lasers," *J. Appl. Phys.*, vol. 49, pp. 4644-4648, Sept. 1978.

[11] R. Adler, "A study of locking phenomena in oscillators," *Proc. IRE*, vol. 34, pp. 351-357, Oct. 1946.

[12] S. Kobayashi and T. Kimura, "Gain and saturation power of resonant AlGaAs laser amplifier," *Electron. Lett.*, vol. 16, pp. 230-232, Mar. 1980.

[13] C. J. Buczek and R. J. Freiberg, "Hybrid injection locking of higher power CO_2 lasers," *IEEE J. Quantum Electron.*, vol. QE-8, pp. 641-650, July 1972.

[14] S. Kobayashi, Y. Yamamoto, M. Ito, and T. Kimura, "Direct frequency modulation in AlGaAs semiconductor lasers," this issue, pp. 428-441.

[15] K. Otsuka and S. Tarucha, "Theoretical studies on injection locking and injection-induced modulation of laser diodes," *IEEE J. Quantum Electron.*, vol. QE-17, pp. 1515-1521, Aug. 1981.

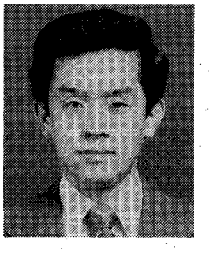

Soichi Kobayashi (M'80) was born in Tokyo, Japan, on January 14, 1947. He received the B.S. and M.S. degrees in electrical engineering from Keio University, Kanagawa, Japan, in 1969 and 1971, respectively.

He joined the Musashino Electrical Communication Laboratory, Nippon Telegraph and Telephone Public Corporation, Tokyo, Japan, in 1971, where he has been engaged in research of the Gunn effect device and optical fiber fabrication. He is presently engaged in research on the characteristics of semiconductor lasers.

Mr. Kobayashi is a member of the Japan Society of Applied Physics and of the Institute of Electronics and Communication Engineers of Japan.

Tatsuya Kimura (S'63-M'68-SM'78), for a photograph and biography, see p. 64 of the January 1982 issue of *IEEE J. Quantum Electron.*